Polyhedron 93 (2015) 99–105

Contents lists available at ScienceDirect

Polyhedron

journal homepage: www.elsevier.com/locate/poly

Mono- and dioxido-vanadium(V) complexes of a tridentate ONO Schiff base ligand: Synthesis, spectral characterization, X-ray crystal structure, and anticancer activity

S. Yousef Ebrahimipour [a,*], Iran Sheikhshoaie [a], Anna Christin Kautz [b], Mojgan Ameri [a], Hamzeh Pasban-Aliabadi [c], Hadi Amiri Rudbari [d], Giuseppe Bruno [e], Christoph Janiak [b]

[a] Department of Chemistry, Faculty of Science, Shahid Bahonar University of Kerman, Kerman, Iran
[b] Institut für Anorganische Chemie und Strukturchemie, Heinrich-Heine-Universität Düsseldorf, Universitätsstr. 1, D-40225 Düsseldorf, Germany
[c] Exercise Physiology Research Center, Baqiyatallah University of Medical Science, Tehran, Iran
[d] Faculty of Chemistry, University of Isfahan, Isfahan 81746-73441, Iran
[e] Università degli Studi di Messina, dip. Scienze Chimiche, Viale Ferdinando S. d'Alcontres, 98166 Messina, Italy

ARTICLE INFO

Article history:
Received 7 January 2015
Accepted 21 March 2015
Available online 7 April 2015

Keywords:
Oxido-vanadium(V) complex
ONO Schiff base ligand
Crystal structure
Anticancer activity
Cell viability

ABSTRACT

Three oxido-vanadium(V) complexes, $[VO_2(L)][NH(Et)_3]$ (**1**), [VO(L)(PrO)] (**2**) and [VO(L)(BuO)] (**3**), containing deprotonated form of the tridentate Schiff base ligand 1-(((5-chloro-2-oxidophenyl) imino)methyl)naphthalen-2-olate $[L^{2-}]$ have been synthesized and characterized using elemental analysis, molar conductivity, FTIR, ^{1}H NMR analysis, and electronic spectroscopy. The structures of the free H_2L ligand and all the complexes were determined by single crystal X-ray diffraction. According to the spectroscopic and structural data, H_2L exists in the solid state in a zwitterionic form. In all the complexes, the V(V) center is coordinated by the ONO donor set of the L^{2-} ligand, one or two oxido groups and in the case of **2** and **3** by one alkoxide group (PrO^- for **2** and BuO^- for **3**) in a distorted square pyramidal geometry. The anticancer activities of the title complexes have been also investigated against MCF-7 (breast cancer) cells and compared with that of $VO(acac)_2$. According to the obtained results, all the complexes possess higher anticancer activity than $VO(acac)_2$.

1. Introduction

Schiff base ligands as privileged ligands have attracted considerable attention due to their facile synthesis and different ligating behavior towards metal ions, as well as significant properties in various fields [1–5]. In addition, vanadium and its Schiff base complexes have received more attention since they can play an important role in bioinorganic chemistry and catalytic processes [6–8]. Although inorganic vanadium salts have considerable toxicity and low biological activity, recent research shows that the complexation of vanadium with organic ligands minimizes the adverse effects and usually increases the important benefits [9].

Vanadium compounds have several pharmacological and physiological roles, such as insulin-mimetic action [10], anti-hypertension, anti-hyperlipidemia [11], anti-obesity [12], enhancement of oxygen affinity of hemoglobin and myoglobin [13], and diuretic action [11]. The anticancer effects of vanadium compounds have been widely investigated on experimental carcinogenesis and tumor-bearing animals [14]. There is also some evidence that vanadium accumulates in cancerous cells and tissues more than normal ones [15,16].

Cancer is a fatal disease and the second leading cause of death in developing countries, so it is critical to find useful ways to defeat this health hazard. Breast cancer is a well-known cancer and is the main cause of cancer deaths in woman throughout the world [17]. MCF-7 cells are useful for in vitro breast cancer studies because the cell line has retained several ideal characteristics particular to the mammary epithelium. These include the ability of MCF-7 cells to process estrogen in the form of estradiol via estrogen receptors in the cell cytoplasm. This makes the MCF-7 cell line an estrogen receptor (ER) positive control cell line [18].

Increasing resistance to multiple drugs is a common clinical problem in the treatment of various cancers. In addition, many current therapeutic procedures have shown multiple side effects [19]. Therefore, it is an immediate requirement to improve anti-cancer

* Corresponding author at: Department of Chemistry, Faculty of Science, Shahid Bahonar University of Kerman, 76169-14111 Kerman, Iran. Tel./fax: +98 34 3132 2143.
E-mail addresses: Ebrahimipour@uk.ac.ir, Ebrahimipour@ymail.com (S.Y. Ebrahimipour).

http://dx.doi.org/10.1016/j.poly.2015.03.037
0277-5387/

therapeutics that effectively and specifically target tumor cells while minimizing the toxic side effects on physiologically proliferating cells. Low dose clinical trials have proven to have minimal side effects, thus an interesting future direction of research can be the development of new drugs with improved anticancer effects in low dose due to the decreased side effects [20].

Here, a tridentate ONO Schiff base ligand [H_2L] and its oxidovanadium(V) complexes have been synthesized and characterized. Moreover, their anticancer activities have been investigated against breast cancer.

2. Experimental

2.1. Materials and instrumentation

All chemicals and solvents used were of analytical reagent grade and were used as received. Microanalyses for C, H and N were determined on a Thermo Finnigan Flash Elemental Analyzer 1112EA. Melting points were measured on an Electrothermal Apparatus-9100. FT-IR spectra were recorded on a Bruker-Tensor 27 as KBr discs in the range 400–4000 cm^{-1}. Molar conductance measurements were made by means of a Metrohm 712 Conductometer in EtOH. ^1H NMR and electronic spectra were recorded at 25 °C on Bruker Avance III 300 and Cary 50 UV–Vis spectrophotometers, respectively. Cell culture reagents, penicillin–streptomycin solution, trypsin EDTA and fetal bovine serum (FBS) were obtained from Biosera Co. (East Sussex, UK). Culture flasks and dishes were acquired from SPL lifesciences Inc (Gyeonggi-Do, South Korea). 3-[4,5-Dimethyl-2-thiazolyl]-2, 5-diphenyl-2-tetrazolium bromide (MTT) was purchased from Sigma (St. Louis, MI, USA).

2.1.1. Synthesis of 1-(((5-chloro-2-hydroxyphenyl)imino)methyl)naphthalen-2-ol [H_2L]

A 3 ml ethanolic solution of 2-amino-4-chlorophenol (2.0 mmol, 0.29 g) was added to an ethanolic solution of 2-hydroxy naphthaldehyde (2.0 mmol, 0.34 g) while stirring vigorously. The obtained orange mixture was refluxed for 30 min. After cooling, the resulting precipitates were filtered off, washed with cold ethanol and dried in a desiccator over $CaCl_2$.

Yield: 0.51 g, 86%. M.p.: 184 °C. *Anal.* Calc. for $C_{17}H_{12}ClNO_2$ (297.74 g mol^{-1}): C, 68.58; H, 4.06; N, 4.70. Found: C, 68.18; H, 4.31; N, 7.53%. FT-IR (KBr), cm^{-1}: ν(OH) 3314, ν(NH) 3033, ν(C=O) 1683, ν(C=N) 1620, ν(C=C_{ring}) 1543, ν(C—O) 1345, δ_{oopb}(OH) 743, ν(C—Cl) 681. ^1H NMR (300 MHz, DMSO-d_6, 25 °C, ppm) δ: 15.63 (s, 1H; OH), 10.57 (s, 1H; OH), 9.52 (s, 1H; CH=N), 6.77–8.46 (m, 9H, aryl rings). UV–Vis (EtOH) λ_{max}, nm (log ε, L mol^{-1} cm^{-1}): 262 (4.98), 325 (4.13), 372 (3.87), 456 (4.31), 478 (4.29).

2.1.2. Synthesis of triethylammonium-1-(((5-chloro-2-oxidophenyl)imino)methyl) naphthalen-2-olate-di-oxido-vanadate(V) [$NH(CH_2CH_3)_3$][VO_2(L)] (**1**)

To a solution of H_2L (0.4 mmol, 0.12 g) in ethanol (5 ml), triethylamine (0.8 mmol, 0.12 ml) was added with constant stirring. Then, 3 ml of an ethanolic solution of $VO(acac)_2$ (0.4 mmol, 0.12 g) was added to the mixture and the obtained brown solution was refluxed in an oil bath for 10 min. Brown crystals were obtained by slow evaporation of the mother liquor after 2 days at room temperature.

Yield: 0.14 g, 73%. M.p.: 232 °C. Molar conductance (1×10^{-3} M, EtOH): 97 Ω^{-1} cm^2 mol^{-1}. *Anal.* Calc. for $C_{23}H_{26}ClN_2O_4V$ (480.86 g mol^{-1}): C, 57.54; H, 5.45; N, 5.83. Found: C, 57.49; H, 5.38; N, 5.90%. FT-IR (KBr), cm^{-1}: ν(N—H) 3001, ν(C=N) 1616, ν(C=C_{ring}) 1534, ν(C—O) 1296, ν(V=O) 989, ν(C—Cl) 684, ν(V—O) 574, ν(V—N) 476. ^1H NMR (300 MHz, DMSO-d_6, 25 °C, ppm) δ: 10.02 (s, 1H; CH=N), 8.87 (br, 1H, NH), 6.65–8.73 (m, 9H, rings), 3.08 (q, 6H, CH_2), 1.15 (t, 9H, CH_3). UV–Vis (EtOH) λ_{max}, nm (log ε, L mol^{-1} cm^{-1}): 287 (4.35), 338 (4.21), 461 (4.30).

2.1.3. Synthesis of 1-(((5-chloro-2-oxidophenyl)imino)methyl)-naphthalen-2-olate-propoxido-oxido-vanadium(V) [VO(L)(PrO)] (**2**)

$VO(acac)_2$ (0.4 mmol, 0.12 g) was added to a solution containing an equimolar quantity of H_2L (0.12 g) in 6 ml of boiling propanol and the resulting mixture was refluxed in an oil bath for 30 min. After cooling, the solid formed was separated, washed with cold propanol and dried in a vacuum desiccator over $CaCl_2$.

Yield: 0.12 g, 71%. M.p.: 206 °C. Molar conductance (1×10^{-3} M, EtOH): 4 Ω^{-1} cm^2 mol^{-1}. *Anal.* Calc. for $C_{20}H_{17}ClNO_4V$ (421.75 g mol^{-1}): C, 56.96; H, 4.06; N, 3.32. Found: C, 56.93; H, 4.15; N, 3.38%. FT-IR (KBr), cm^{-1}: ν(C=N) 1599, ν(C=C_{ring}) 1534, ν(C—O) 1297, ν(V=O) 999, ν(C—Cl) 685, ν(V—O) 566, ν(V—N) 478. ^1H NMR (300 MHz, DMSO-d_6, 25 °C, ppm) δ: 9.98 (9.88) (s, 1H; CH=N), 6.67–8.77 (m, 18H, rings), 5.61 (m, 3H, OH, CH_2), 3.43 (m, 2H, CH_2), 1.89 (m, 2H, CH_2), 1.86 (m, 2H, CH_2), 1.01 (d, 3H, CH_3), 0.91 (d, 2H, CH_3). UV–Vis (EtOH) λ_{max}, nm (log ε, L mol^{-1} cm^{-1}): 280 (4.37), 339 (4.17), 461 (4.20).

2.1.4. Synthesis of 1-(((5-chloro-2-oxidophenyl)imino)methyl)-naphthalen-2-olate-butoxido-oxido-vanadium(V) [VO(L)(BuO)] (**3**)

The preparation procedure for this complex is similar to that for **2**, except butanol was used as the solvent. The formed clear brown solution was filtered and left to stand overnight. Orange crystals were separated after slow evaporation at room temperature for 3 days, and they were dried in a desiccator over $CaCl_2$.

Yield: 0.13 g, 74%. M.p.: 211 °C. Molar conductance (1×10^{-3} M, EtOH): 8 Ω^{-1} cm^2 mol^{-1}. *Anal.* Calc. for $C_{21}H_{19}ClNO_4V$ (435.77 g mol^{-1}): C, 57.88; H, 4.39; N, 3.21. Found: C, 57.81; H, 4.43; N, 3.27%. FT-IR (KBr), cm^{-1}: ν(C=N) 1598, ν(C=C_{ring}) 1535, ν(C—O) 1289, ν(V=O) 981, ν(C—Cl) 683, ν(V—O) 571, ν(V—N) 464. ^1H NMR (300 MHz, DMSO-d_6, 25 °C, ppm) δ: 9.99 (9.89) (s, 1H; CH=N), 6.68–8.77 (m, 18H, rings), 5.68 (s, 1H, OH), 5.58 (t, 2H, CH_2), 3.38 (m, 2H, CH_2), 1.84 (m, 2H, CH_2), 1.56 (m, 2H, CH_2), 1.43 (m, 2H, CH_2), 1.37 (m, 2H, CH_2), 0.94 (t, 3H, CH_3), 0.81 (t, 3H, CH_3). UV–Vis (EtOH) λ_{max}, nm (log ε, L mol^{-1} cm^{-1}): 267 (4.05), 353 (3.72), 464 (3.86).

2.2. Crystal structure determination

Crystallographic data (room temperature for the ligand, compound **1** and **2**; 100 K for compound **3**) were collected with a Bruker Kappa APEX II CCD area detector diffractometer using Mo Kα radiation (λ = 0.71073 Å). Data collection was performed using APEX2 [21], cell refinement and data reduction using SAINT (Bruker) [21]. The structures were solved by direct methods (SHELXS-97) [22], refinement was done by full-matrix least squares on F^2 using the SHELXL-97 program suite, empirical (multi-scan) absorption correction using SADABS (Bruker) [23]. All the hydrogen atoms, except hydrogens of oxygen and nitrogen atoms, were placed at calculated positions and constrained to ride on their parent atoms. Hydrogen atoms for aromatic CH, CH_2 and methyl groups were positioned geometrically (C—H = 0.93 Å for aromatic CH, C—H = 0.97 Å for CH_2, C—H = 0.96 Å for CH_3) and refined using a riding model (AFIX 43 for aromatic CH, AFIX 23 for CH_2 AFIX 33 or rotating group refinement 137 for CH_3), with $U_{iso}(H) = 1.2\,U_{eq}(CH)$ and $U_{iso}(H) = 1.5\,U_{eq}(CH_3)$. H atoms on oxygen and nitrogen atoms in compounds **1** and **2** were found in difference Fourier maps and refined isotropically. In compound **2**, the C19 atom of the

1-propanolate group was disordered and split over two positions (75:25 occupancy for C19 and C19′, respectively). Also, in compound **1** the C20 atom of the protonated triethylamine was disordered and split over two positions, (54:46 occupancy for C20 and C20′, respectively). Details concerning collection and analysis are reported in Table 1.

2.3. Cell culture

MCF-7 (breast cancer) cells were obtained from the National Cell Bank of Iran (NCBI) – Pasteur Institute of Iran (Tehran, Iran). Cells were grown with Dulbecco's modified Eagle's medium supplemented with 10% fetal bovine serum, penicillin (100 U/ml) and streptomycin (100 g/ml). They were maintained at 37 °C in a 5% CO_2 atmosphere. The growth medium was changed three times a week. Cells were plated at a density of 5000 per well in a 96 micro plate well for the MTT assay. The cells were incubated with different doses of $VO(acac)_2$ and the title complexes.

2.4. Cell viability analysis

2.4.1. MTT assay

Cellular viability was assessed by the reduction of 2-(4, 5-dimethylthiazol-2-yl)-2,5-diphenyltetrazolium bromide (MTT) to formazan [24]. The reduction of tetrazolium salts is now widely accepted as a reliable way to examine cell proliferation. The yellow tetrazolium MTT (3-(4,5-dimethylthiazolyl-2)-2,5-diphenyltetrazolium bromide) is reduced by metabolically active cells, in part by the action of dehydrogenase enzymes, to generate reducing equivalents such as NADH and NADPH. The resulting intracellular purple formazan can be solubilized and quantified by spectrophotometric means [24]. MTT was dissolved in PBS and added to the culture at a final concentration of 0.5 mg/ml. After an additional 2 h incubation at 37 °C, the media were carefully removed and 100 µl DMSO was added to each well, and the absorbance (OD) values were determined by spectrophotometry at 490 nm with a microplate reader (BioTek ELX808). The results were expressed as percentages of the control.

2.4.2. Statistical analysis

The results are expressed as mean ± SEM. The differences in cell viability (mean MTT assay) between groups were determined by one-way ANOVA, followed by the Tukey test. $P < 0.05$ was considered significant.

3. Results and discussion

Three new oxido-vanadium(V) complexes were prepared by the reaction of equimolar amounts of the tridentate Schiff base ligand [H_2L] and $VO(acac)_2$ in the appropriate solvents. All of the synthesized compounds are stable at room temperature. They are soluble in DMSO, DMF and ethanol, less soluble in other common solvents like dichloromethane and acetonitrile, and are insoluble in benzene and *n*-hexane. The molar conductivity value of complex **1** in EtOH shows that it is a 1:1 type electrolyte, while the low molar conductance values of complexes **2** and **3** solutions in EtOH indicate that these complexes are non-electrolytes.

3.1. Spectral characterization

3.1.1. FTIR study

Selected frequencies and vibrational assignments of H_2L and its oxido-vanadium(V) complexes are listed in the experimental section. In the spectrum of the ligand, the bands at 3314 and 743 cm^{-1} are assigned to stretching and out of plane bending of OH, respectively [25]. Upon coordination, these bands disappear,

Table 1
Crystal data and structure refinement for H_2L and its V(V) complexes.

	H_2L	1	2	3
Empirical formula	$C_{17}H_{12}ClNO_2$	$C_{23}H_{26}ClN_2O_4V$	$C_{20}H_{17}ClNO_4V$	$C_{21}H_{19}ClNO_4V$
Formula weight (g mol^{-1})	297.73	480.85	421.74	435.76
T (K)	298(2)	298(2)	298(2)	100(2)
Crystal system	triclinic	monoclinic	triclinic	triclinic
Space group	$P\bar{1}$	$P2_1/n$	$P\bar{1}$	$P\bar{1}$
Unit cell dimensions				
a (Å)	7.3133(2)	7.8052(2)	8.1384(4)	8.3432(11)
b (Å)	7.8799(2)	14.4648(4)	9.7071(4)	11.2706(14)
c (Å)	13.6546(3)	19.7036(5)	12.2441(6)	11.6151(15)
α (°)	88.9620(10)	90	81.571(2)	63.781(3)
β (°)	74.6290(10)	95.2780(10)	84.969(2)	74.413(3)
γ (°)	63.8790(10)	90	75.804(2)	76.156(3)
V ($Å^3$)	676.82(3)	2215.12(10)	926.27(7)	934.6(2)
Z	2	4	2	2
Density (Calc., mg/m^3)	1.461	1.442	1.512	1.549
Absorption coefficient (mm^{-1})	0.285	0.601	0.706	0.702
$F(000)$	308	1000	432	448
θ range (°)	2.90–26.49	2.51–25.00	2.59–27.00	2.19–24.49
Limiting indices	$-9 \leqslant h \leqslant 9$ $-9 \leqslant k \leqslant 9$ $-17 \leqslant l \leqslant 17$	$-9 \leqslant h \leqslant 9$, $-17 \leqslant k \leqslant 17$ $-23 \leqslant l \leqslant 23$	$-10 \leqslant h \leqslant 10$ $-12 \leqslant k \leqslant 12$ $-15 \leqslant l \leqslant 15$	$9 \leqslant h \leqslant 9$ $-13 \leqslant k \leqslant 13$ $-13 \leqslant l \leqslant 13$
Reflections collected/unique	21 879/2793 [R_{int} = 0.0362]	82 757/3888 [R_{int} = 0.0746]	19 108/3975 [R_{int} = 0.0486]	7880/3102 [R_{int} = 0.0372]
Compl. (%) to θ_{full} (°)	99.9;26.49	99.7; 25.00	98.1; 27.00	99.3; 24.52
Data/restraints/parameters	2793/0/198	3888/0/290	3975/2/254	3102/0/254
Goodness-of-fit on F^2[a]	1.026	1.054	1.006	1.041
R_1/wR_2 [$I > 2\sigma(I)$] [b]	0.0372/0.0955	0.0511/0.1196	0.0435/0.0932	0.0316/0.0770
R_1/wR_2 (all reflections)[b]	0.0567/0.1090	0.0793/0.1370	0.0813/0.1091	0.0402/0.0812
Largest difference peak and hole (e $Å^{-3}$)[c]	0.254 and −0.197	0.381 and −0.395	0.312 and −0.255	0.411 and −0.250

[a] Goodness-of-fit = $[\Sigma[w(F_0^2 - F_c^2)^2]/(n-p)]^{1/2}$.
[b] $R_1 = [\Sigma(||F_o| - |F_c||)/\Sigma|F_o|]$; $wR_2 = [\Sigma[w(F_0^2 - F_c^2)^2]/\Sigma[w(F_0^2)^2]]^{1/2}$.
[c] Largest difference peak and hole.

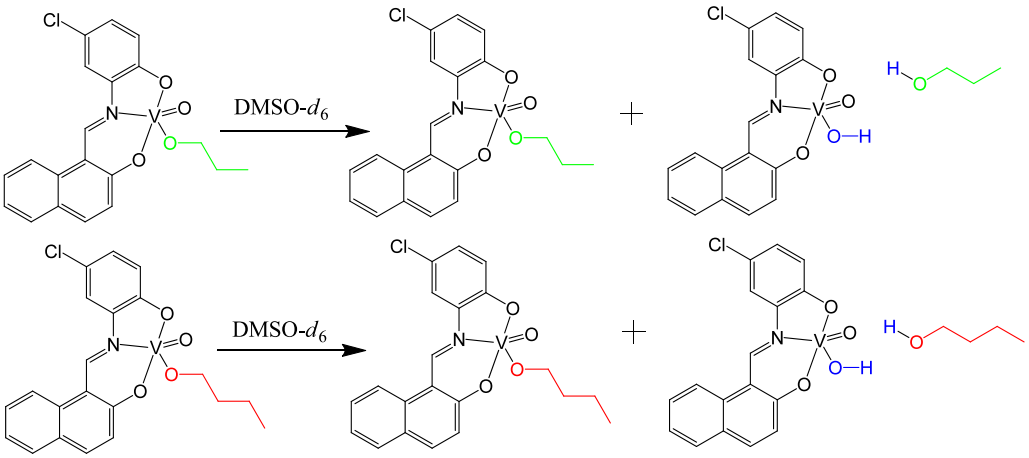

Fig. 1. Schematic diagram for the cleavage of the complexes in DMSO-d_6.

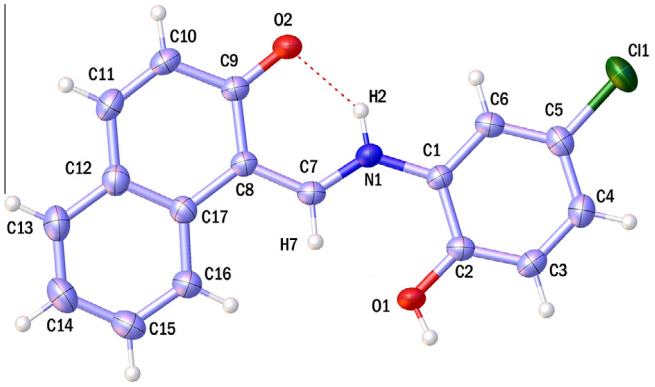

Fig. 2. Structure of the zwitterionic ligand H_2L (50% thermal ellipsoids; H atoms at arbitrary radii). The charge-assisted intramolecular (imine)N–$H^+\cdots^-$O(naphthol) interaction is shown as a dashed red line. (Colour online.)

which is consistent with the coordination of the Schiff base to the vanadium center through the deprotonated phenolic oxygens. In H_2L, the bands observed at 3033 and 1683 cm^{-1} correspond to NH and C=O vibrations, respectively and show that the free ligand exists in the *keto-amine* (*quinoid*) form [6]. After complexation, the absence of these bands is an evidence of ligand coordination to the central ion in the *enol-imine* (*benzenoid*) form. In **1**, the absorption band at 3001 cm^{-1} is correlated to the vibration of NH corresponding to triethylammonium. In the spectrum of the ligand, the strong band at 1620 cm^{-1} is related to the vibration of the azomethine moiety, and its red shift observed in the spectra of all complexes indicate the azomethine nitrogen atoms coordinate to the metal center [26]. The vibration of CO is disclosed as a medium band at 1300 cm^{-1} in the free ligand, which exhibits displacements of 4, 3 and 11 cm^{-1} to lower frequencies in complexes **1**, **2** and **3**, respectively [27]. These shifts support the coordination of the phenolic oxygen atoms to the vanadium centers. The bands appearing in the range 999–981 cm^{-1} correspond to ν(V=O) of the vanadyl moiety [28]. The medium band at 1543 cm^{-1} in the spectrum of the Schiff base ligand is ascribed to a C=C vibration. For complexes, this vibration appears in the range 1534–1535 cm^{-1} [29].

3.1.2. Electronic spectra

The electronic spectra of the compounds were obtained in EtOH at room temperature. In the electronic spectrum of the free

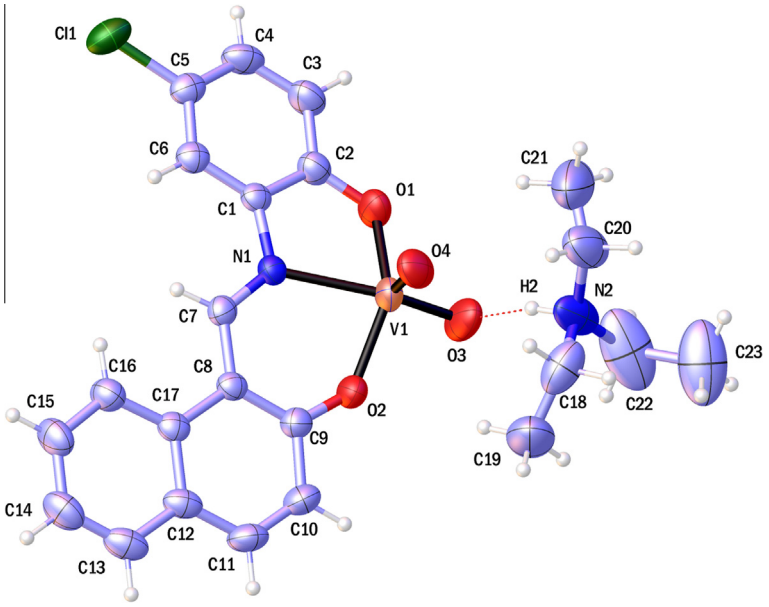

Fig. 3. ORTEP representation of **1**. Displacement ellipsoids are drawn at the 50% probability level and H atoms are shown as small spheres of arbitrary radii. C20 of protonated triethylamine is disordered and split over two positions but the disorder is not shown for clarity.

ligand, the absorption band at 262 nm is assigned to the $\pi\rightarrow\pi^*$ transition of the aromatic rings. The other transition bands observed in the range of 325–478 nm correspond to $\pi\rightarrow\pi^*$ and $n\rightarrow\pi^*$ transitions of the azomethine moiety, respectively [28]. In the UV–Vis spectra of the complexes, the bands at approximately 461 nm are assigned to N(P)/O(p)→V(d) charge transfers (LMCT). The other bands can be correlated to $\pi\rightarrow\pi^*$ intra-ligand transitions [6].

3.1.3. ^{1}H NMR study

The ^{1}H NMR spectra of the synthesized compounds were recorded in DMSO-d_6 (Fig. S1). In the ^{1}H NMR spectrum of the ligand, singlet signals at 15.63 and 10.57 ppm are ascribed to OH protons (*enol-imine* form) [30]. Intermolecular hydrogen bonding, resulting in the formation of six- and five-membered rings, is the main reason for the deshielding of these protons [28]. After complexation, the disappearance of these signals indicates coordination through deprotonated hydroxyl groups. Moreover, the protons of the aromatic rings are disclosed as multiplets in the range 6.78–8.46 ppm. The azomethine proton is observed at 9.52 ppm in the spectrum of the ligand, whereas in the ^{1}H NMR spectra of the complexes, this proton shows a significant downfield shift which is consistent with the coordination of the azomethine nitrogen atom to the metal ion. Analyzing the spectrum of complex **1** reveals the presence of NH as a broad band at 8.87 ppm. The methyl and methylene protons of the triethyl ammonium moiety appear at 1.15 and 3.08 ppm, respectively. However, the ^{1}H NMR spectra of complexes **2** and **3** in DMSO-d_6 show the existence of two different complexes; the title complexes and their cleavage products. In other words, replacement of the alkoxide group by an hydroxy group results in the production of a second complex with the structure depicted in Fig. 1.

3.1.4. X-ray crystal structure

The molecular structures of the ligand H_2L and complexes **1**, **2** and **3** with the atom numbering are shown in Figs. 2–5, respectively. The ligand H_2L shows the expected constitution, except that the naphthol group is deprotonated to give a zwitterion with an intramolecular (imine)N—H$^+\cdots^-$O (naphthol) hydrogen bond (*keto-amine* form). Deprotonation of the phenol group and

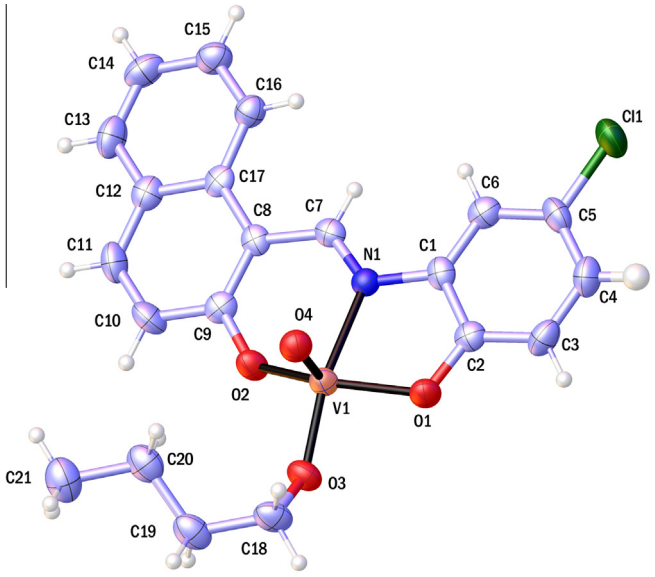

Fig. 5. ORTEP representation of **3**. Displacement ellipsoids are drawn at the 50% probability level and H atoms are shown as small spheres of arbitrary radii.

Table 2
Selected bond lengths (Å) and angles (°) for the zwitterionic ligand H_2L with esd's in parentheses.

Bond length	
O1–C2	1.3447(19)
O2–C9	1.2833(18)
N1–C7	1.314(2)
N1–C1	1.4098(19)
Cl1–C5	1.7366(17)
Bond angle	
N1–C7–C8	123.66(13)
C7–N1–C1	129.70(13)
C8–C9–O2	121.67(13)
C1–C2–O1	118.72(14)
N1–C1–C2	124.09(14)
C7–C8–C9	120.23(14)

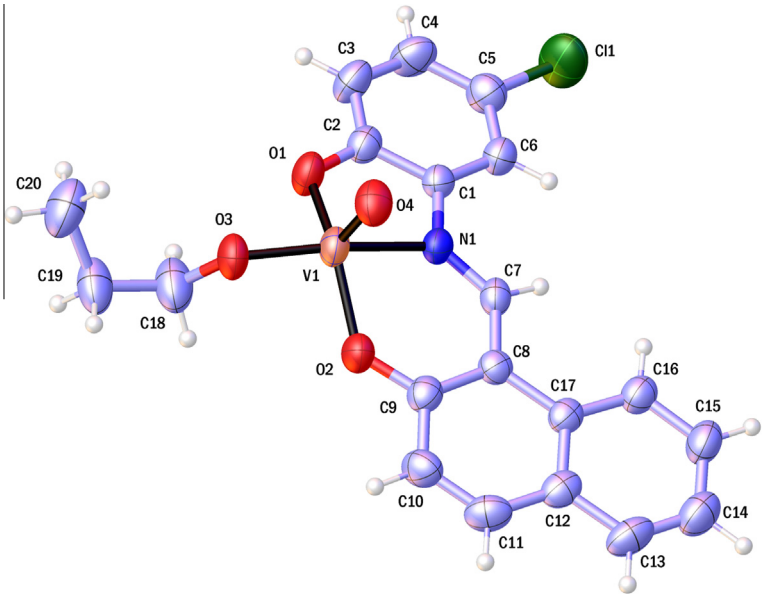

Fig. 4. ORTEP representation of **2**. Displacement ellipsoids are drawn at the 50% probability level and H atoms are shown as small spheres of arbitrary radii. C19 is disordered and split over two positions but the disorder is not shown for clarity.

protonation of the imine nitrogen in salicylaldimine-type compounds to give a zwitterion is rare [31–34] in view of the vast number of salicylaldimine derivatives, yet such an intramolecular shift of the H atom from (imine) N···H—O (phenol-type) (*enol-imine* form) to (imine)N—$H^{+}\cdots^{-}$O (phenol-type) (*keto-amine* form) is assumed as the first step in the catalytic cycle of enzymatic transformations of amino acids with the cofactor (vitamin B6) pyridoxal-5′-phosphate (PLP). This intramolecular hydrogen transfer is assisted by the protonation of the pyridine ring, which enhances the electric field [28].

This zwitterionic constitution is supported by the bond lengths: the naphtholate C9—O2^{-} bond length of 1.2833(18) Å corresponds to a C=O double bond because of the charge delocalization into the naphthyl system, whereas the phenol C2—O1(—H) bond of 1.3447(19) Å is within the limits of a C—O single bond (Table 2) [35].

The packing of the ligand is dominated by "charge-assisted" hydrogen bonds, wherein the hydrogen bond donor and/or acceptor carry positive and negative ionic charges, respectively [36–39]. The enhancement of the hydrogen bond strength, which may be linked to robustness, by ionic charge has long been recognized and some of the strongest hydrogen bonds are "charge-assisted". In the structure of H_2L there is one intermolecular O—H···$^{-}$O and one intramolecular N—$H^{+}\cdots^{-}$O hydrogen bond (Figs. S2 and 2 respectively, Table 3).

In the structure of the anionic part of **1**, the vanadium atom is pentacoordinated by two oxido groups and the dianionic tridentate ONO Schiff base ligand. The two oxido oxygen atoms are in a *cis*-position. The 1-(((5-chloro-2-oxidophenyl)imino)methyl)naphthalen-2-olate [L^{2-}] coordinates through the imino nitrogen atom and the two phenolate and naphtholate oxygen atoms. The vanadium coordination sphere is a slightly distorted square–pyramid, as ascertained by the structural parameter $\tau = 0.29$ (0 for an ideal square pyramid and 1 for an ideal trigonal bipyramid) [40].

The crystal structures of **2** and **3** consist of a vanadium atom pentacoordinated by an oxido group, one alkoxide (propoxide for **2** and butoxide for **3**) and the dianionic tridentate ONO Schiff base ligand. In both structures the oxido oxygen atom is in a *cis*-position to the alkoxide group. The Schiff base ligand coordinates as seen in the structure of **1**. Again in both structures the vanadium coordination sphere is a distorted square–pyramid, as ascertained by the structural parameter $\tau = 0.34$ for **2** and 0.29 for **3**.

Selected geometrical parameters for complexes **1**–**3** are listed in Table 4. The oxido function V=O (V1–O4) of compounds **2** and **3** shows bond distances of 1.5835(19) (**2**) and 1.5931(15) Å (**3**). The distances are only slightly shorter and rather similar to those found in other $V^{V}O$-complexes with a square pyramidal VO_4N environment [6,41,42]. The vanadium alkoxido (V1—O3) bond distances, 1.7700(18) (**2**) and 1.7609(15) Å (**3**) are as expected from the related isopropoxy compounds ^{i}PrO(VO) (Schiff-base ligands) [43].

Also the V—N (imine) bond lengths (V1—N1) are in the range found for other pentacoordinated V(=O) Schiff base complexes [6,28]. The supramolecular weak π–π interactions and intermolecular C–H···O interactions in the packing of the ligand H_2L and compounds **1**–**3** are analyzed and detailed in the Supporting information. There are no C—H···π interactions or C—H···Cl interactions in the packing of these compounds.

Table 3
Hydrogen bonds in the crystal structure of H_2L.

D—H···A	D—H (Å)	H···A (Å)	D···A (Å)	D—H···A (°)	Symmetry
O1—H1…O2[a]	0.82(2)	1.76(2)	2.5630(18)	167(2)	$x, -1+y, z$
N1— H2…O2	0.87(2)	1.85(2)	2.5880(18)	141(2)	x, y, z

[a] The intermolecular hydrogen bond is shown in Fig. S2 in the Supporting information.

Table 4
Selected bond lengths (Å) and angles (°) for **1**, **2** and **3** with esd's in parentheses.

Compound	**1**	**2**	**3**
V1–O1	1.920(3)	1.881(2)	1.8777(15)
V1–O2	1.904(2)	1.8503(19)	1.8592(14)
V1–O3	1.638(3)	1.7700(18)	1.7609(15)
V1–O4	1.630(3)	1.5835(19)	1.5931(15)
V1–N1	2.189(3)	2.122(2)	2.1502(18)
O1–C2	1.333(4)	1.340(3)	1.337(3)
O2–C9	1.311(4)	1.329(3)	1.322(3)
N1–C7	1.289(4)	1.302(3)	1.303(3)
N1–C1	1.425(4)	1.423(3)	1.421(3)
O4–V1–O3	106.19(18)	105.73(10)	105.36(7)
O4–V1–O2	106.99(13)	108.21(10)	107.36(7)
O4–V1–O1	108.24(13)	110.33(10)	105.90(7)
O4–V1–N1	96.39(13)	95.60(9)	95.53(7)
O3–V1–O1	94.03(14)	90.02(9)	94.51(7)
O3–V1–O2	94.24(14)	95.62(9)	94.47(7)
O2–V1–N1	80.59(10)	82.36(8)	80.82(6)
O1–V1–N1	76.86(10)	77.47(8)	77.65(6)
O2–V1–O1	139.79(12)	137.80(9)	141.72(7)
O3–V1–N1	157.34(16)	158.04(9)	159.03(7)

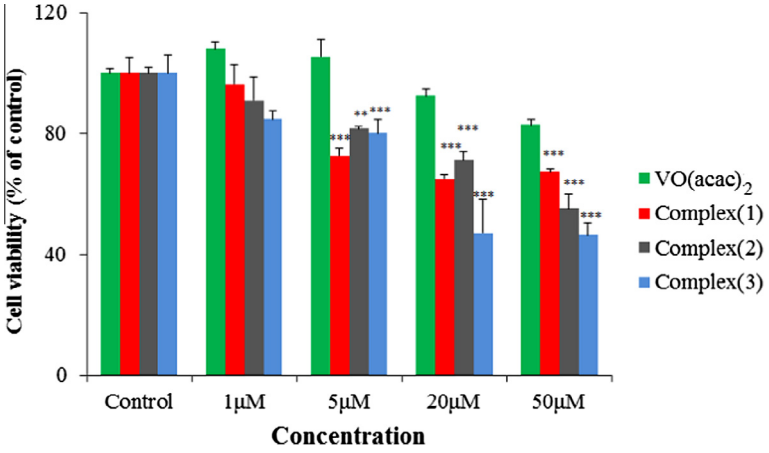

Fig. 6. Effect of different doses of vanadium and the vanadium complexes on MCF-7 cancer cells viability determined by an MTT assay. The component has a dose dependent toxic effect on cancer cells. Data are expressed as mean ± SEM; $n = 6$ well for each group; $^{**}P < 0.01$ and $^{***}p < 0.001$ vs. control (non-treated) cells.

3.2. Anticancer activity

The anticancer properties of the compounds (complexes and ligand) the concentration range of 1–20 μM were investigated against MCF-7 breast cancer cells. The cells viability was determined using an MTT assay after 24 h treatment and the obtained results are presented in Fig. 6. The complexes displayed higher anticancer activities than vanadium itself. It has been reported that vanadium is a known anti-cancer agent. However, the oxido-vanadium(V) complexes synthesized here showed significantly higher toxic effects on the cell line in all used concentrations. Especially in low doses the cell viabilities observed in the presence of the complexes were lower than those observed in the presence of $VO(acac)_2$. In the other words, high doses may produce more severe side effects and scientific efforts to achieve the lowest therapeutic dose which produces the desired clinical effect are of intensive interest.

The observed anti-proliferative effects of vanadium complexes can be due to the following mechanisms. Redox-active vanadium compounds can produce high levels of reactive oxygen species (ROS) which disrupts the redox homeostasis in tumor cells and induce redox stress. Such a situation promotes cell apoptosis either by cleaving DNA or facilitating mitochondrial membrane permeability and the release of cytochrome c [44]. Furthermore, vanadium compounds are genotoxic and elicit selective oxidation of pyrimidine bases and single-strand break-type DNA damage in tumor cells which is characterized by less efficient DNA repair processes [45,46].

4. Conclusion

Two mono and one dioxido-vanadium(V) complexes have been prepared and structurally characterized using physico-chemical and spectroscopic methods. Complex **1** has 1:1 electrolyte behavior while the other complexes have a non-electrolytic nature in EtOH. Experimental investigation revealed that H_2L is coordinated to the central ion as a dianionic chelator. Other positions around V(V) center are occupied by oxido groups and the oxygen atom of an alkoxide group (PrO^- for **2** and BuO^- for **3**). According to a biochemical investigation, these complexes have good activity against breast cancer and can be considered as potent anticancer agents. It is shown that the oxido-vanadium(V) complexes decrease cell viability more than $VO(acac)_2$ itself. However, the exact cellular anticancer mechanism(s) of such compounds needs to be clarified in future studies.

Acknowledgements

Authors gratefully acknowledge the financial support provided for this work by the Shahid Bahonar University of Kerman.

Appendix A. Supplementary data

CCDC 1032428, 1032429, 1028790 and 1052671 contains the supplementary crystallographic data for H_2L, **1**, **2** and **3** respectively. These data can be obtained free of charge via http://www.ccdc.cam.ac.uk/conts/retrieving.html, or from the Cambridge Crystallographic Data Centre, 12 Union Road, Cambridge CB2 1EZ, UK. Fax: +44 1223 336 033; or e-mail: deposit@ccdc.cam.ac.uk.

Supplementary data associated with this article can be found, in the online version, at http://dx.doi.org/10.1016/j.poly.2015.03.037.

References

[1] M. Enamullah, A.R. Uddin, G. Pescitelli, R. Berardozzi, G. Makhloufi, V. Vasylyeva, A.-C. Chamayou, C. Janiak, Dalton Trans. 43 (2014) 3313.
[2] M. Enamullah, V. Vasylyeva, C. Janiak, Inorg. Chim. Acta 408 (2013) 109.
[3] S.Y. Ebrahimipour, I. Sheikhshoaie, A. Crochet, M. Khaleghi, K.M. Fromm, J. Mol. Struct. 1072 (2014) 267.
[4] K.C. Gupta, A.K. Sutar, Coord. Chem. Rev. 252 (2008) 1420.
[5] M. Rezaeivala, H. Keypour, Coord. Chem. Rev. 280 (2014) 203.
[6] S.Y. Ebrahimipour, M. Abaszadeh, J. Castro, M. Seifi, Polyhedron 79 (2014) 138.
[7] a) D. Rehder, Inorg. Chem. Commun. 6 (2003) 604;
b) I. Sheikhshoaie, S.Y. Ebrahimipour, A. Crochet, K.M. Fromm, Res. Chem. Intermediat. 41 (2015) 1881.
[8] E. Tsuchida, K. Oyaizu, Coord. Chem. Rev. 237 (2003) 213.
[9] J.H. McNeill, V.G. Yuen, S. Dai, C. Orvig, Mol. Cell. Biochem. 153 (1995) 175.
[10] D. Rehder, J.C. Pessoa, C.F. Geraldes, M.M. Castro, T. Kabanos, T. Kiss, B. Meier, G. Micera, L. Pettersson, M. Rangel, J. Biol. Inorg. Chem. 7 (2002) 384.
[11] H. Michibata, Vanadium: Biochemical and Molecular Biological Approaches, Springer, Netherlands, 2011.
[12] S.-J. Park, C.-K. Youn, J.W. Hyun, H.J. You, Biol. Trace Elem. Res. 151 (2013) 294.
[13] B. Mukherjee, B. Patra, S. Mahapatra, P. Banerjee, A. Tiwari, M. Chatterjee, Toxicol. Lett. 150 (2004) 135.
[14] A.M. Evangelou, Crit. Rev. Oncol. Hematol. 42 (2002) 249.
[15] A. Bishayee, A. Waghray, M.A. Patel, M. Chatterjee, Cancer Lett. 294 (2010) 1.
[16] I. Kostova, Anti-Cancer Agents Med. Chem. 9 (2009) 827.
[17] R. Siegel, D. Naishadham, A. Jemal, CA Cancer J. Clin. 62 (2012) 10.
[18] A.S. Levenson, V.C. Jordan, Cancer Res. 57 (1997) 3071.
[19] W.T. Beck, Cancer Treat. Rep. 67 (1983) 875.
[20] a) M. Lazzeroni, D. Serrano, B.K. Dunn, B.M. Heckman-Stoddard, O. Lee, S. Khan, A. Decensi, Breast Cancer Res. 14 (2012) 214;
b) M. Hertzman, L. Adler, Clinical Trials in Psychopharmacology: A Better Brain, Second ed., John Wiley & Sons, New York, 2010.
[21] APEX2, SAINT, Bruker, Madison, WI, USA, 2012.
[22] G.M. Sheldrick, Acta Crystallogr., Sect. A 64 (2008) 112.
[23] G.M. Sheldrick, SADBS, University of Göttingen, Göttingen, Germany, 1996.
[24] F. Denizot, R. Lang, J. Immunol. Methods 89 (1986) 271.
[25] S.Y. Ebrahimipour, I. Sheikhshoaie, J. Castro, W. Haase, M. Mohamadi, S. Foro, M. Sheikhshoaie, S. Esmaeili-Mahani, Inorg. Chim. Acta 430 (2015) 245.
[26] (a) R. Takjoo, A. Akbari, S.Y. Ebrahimipour, H. Amiri Rrudbari, G. Brunò, IC. R. Chim. 17 (2014) 1144;
(b) S.Y. Ebrahimipour, M. Mohamadi, J. Castro, N. Mollania, H. Amiri Rudbari, A. Saccá, J. Coord. Chem. 68 (2015) 632;
(c) S.Y. Ebrahimipour, Z. Rashid Ranjabr, E. Tavakolinejad Kermani, B. Pour Amiri, H. Amiri Rudbari, A. Saccá, F. Hoseinzade, Transit. Metal Chem. 40 (2015) 39.
[27] (a) S.Y. Ebrahimipour, H. Khabazadeh, J. Castro, I. Sheikhshoaie, A. Crochet, K.M. Fromm, Inorg. Chim. Acta 427 (2014) 52;
(b) S.Y. Ebrahimipour, I. Sheikhshoaie, M. Mohamadi, S. Suarez, R. Baggio, M. Khaleghi, M. Torkzadeh-Mahani, A. Mostafavi, Spectrochim. Acta, Part A 142 (2015) 410.
[28] S.Y. Ebrahimipour, J.T. Mague, A. Akbari, R. Takjoo, J. Mol. Struct. 1028 (2012) 148.
[29] R. Takjoo, J.T. Mague, A. Akbari, S.Y. Ebrahimipour, J. Coord. Chem. 66 (2013) 2852.
[30] A. Makal, W. Schilf, B. Kamieński, A. Szady-Chelmieniecka, E. Grech, Krzysztof Woźniak, Dalton Trans. 40 (2011) 421.
[31] B.M. Drašković, G.A. Bogdanovic, M. Neelakantan, A.C. Chamayou, S. Thalamuthu, Y.S. Avadhut, J.R. Schmedt auf der Günne, S. Banerjee, C. Janiak, Cryst. Growth Des. 10 (2010) 1665.
[32] N.S. Golubev, S.N. Smirnov, P.M. Tolstoy, S. Sharif, M.D. Toney, G.S. Denisov, H.H. Limbach, J. Mol. Struct. 844–845 (2007) 319.
[33] R. Kannappan, D.M. Tooke, A.L. Spek, J. Reedijk, Inorg. Chim. Acta 359 (2006) 334.
[34] S. Takeda, T. Inabe, C. Benedict, U. Langer, H.H. Limbach, Ber. Bunsenges. Phys. Chem. 102 (1998) 1358.
[35] A.G. Orpen, L. Brammer, F.H. Allen, O. Kennard, D.G. Watson, R. Taylor, J. Chem. Soc., Dalton Trans. (1989) S1.
[36] M.D. Ward, Chem. Commun. 47 (2005) 5838.
[37] F. Zhuge, B. Wu, J. Liang, J. Yang, Y. Liu, C. Jia, C. Janiak, N. Tang, X.J. Yang, Inorg. Chem. 48 (2009) 10249.
[38] I. Imaz, A. Thillet, J.-P. Sutter, Cryst. Growth Des. 7 (2007) 1753.
[39] L. Marín-García, A. Peña-Hueso, A. Flores-Parra, R. Contreras, Cryst. Growth Des. 6 (2006) 969.
[40] A.W. Addison, T.N. Rao, J. Reedijk, J. van Rijn, G.C. Verschoor, J. Chem. Soc., Dalton Trans. (1984) 1349.
[41] S. Mukherjee, T. Weyhermüller, E. Bothe, P. Chaudhuri, Eur. J. Inorg. Chem. (2003) 1956.
[42] a) M. Bashirpoor, H. Schmidt, C. Schulzke, D. Rehder, Chem. Ber. 130 (1997) 651;
b) S. Das, Polyhedron 27 (2008) 517.
[43] P. Plitt, H. Pritzkow, R. Kramer, Dalton Trans. 15 (2004) 2314.
[44] M. Strianese, A. Basile, A. Mazzone, S. Morello, M.C. Turco, C. Pellecchia, J. Cell. Physiol. 228 (2013) 2202.
[45] K. Wozniak, J. Blasiak, Arch. Toxicol. 78 (2004) 7.
[46] J.J. Rodríguez-Mercado, R.A. Mateos-Nava, M.A. Altamirano-Lozano, Toxicol. In Vitro 25 (2011) 1996.